Developmental Biology 445 (2019) 237–244

Contents lists available at ScienceDirect

Developmental Biology

journal homepage: www.elsevier.com/locate/developmentalbiology

Axonal regrowth is impaired during digit tip regeneration in mice

Connor P. Dolan[a], Mingquan Yan[a], Katherine Zimmel[a], Tae-Jung Yang[a], Eric Leininger[b], Lindsay A. Dawson[a], Ken Muneoka[a,b,*]

[a] Department of Veterinary Physiology and Pharmacology, College of Veterinary Medicine and Biomedical Sciences, Texas A & M University, College Station, TX 77843, USA

[b] Department of Cell and Molecular Biology, School of Science and Engineering, Tulane University, New Orleans, LA 70118, USA

ARTICLE INFO

Keywords:
Regeneration
Digit
Peripheral nervous system
Axon
Schwann cell

ABSTRACT

Mice are intrinsically capable of regenerating the tips of their digits after amputation. Mouse digit tip regeneration is reported to be a peripheral nerve-dependent event. However, it is presently unknown what types of nerves and Schwann cells innervate the digit tip, and to what extent these cells regenerate in association with the regenerative response. Given the necessity of peripheral nerves for mammalian regeneration, we investigated the neuroanatomy of the unamputated, regenerating, and regenerated mouse digit tip. Using immunohistochemistry for β-III-tubulin (β3T) or neurofilament H (NFH), substance P (SP), tyrosine hydroxylase (TH), myelin protein zero (P0), and glial fibrillary acidic protein (GFAP), we identified peripheral nerve axons (sensory and sympathetic), and myelinating- and non-myelinating-Schwann cells. Our findings show that the digit tip is innervated by two digital nerves that each bifurcate into a bone marrow (BM) and connective tissue (CT) branch. The BM branches are composed of sympathetic axons that are ensheathed by non-myelinating-Schwann cells whereas the CT branches are composed of sensory and sympathetic axons and are ensheathed by myelinating- and non-myelinating-Schwann cells. The regenerated digit neuroanatomy differs from unamputated digit in several key ways. First, there is 7.5 fold decrease in CT branch axons in the regenerated digit compared to the unampuated digit. Second, there is a 5.6 fold decrease in myelinating-Schwann cells in the regenerated digit compared to the unamputated digit that is consistent with the decrease in CT branch axons. Importantly, we also find that the central portion of the regenerating digit blastema is aneural, with axons and Schwann cells restricted to peripheral and distal blastema regions. Finally, we show that even with impaired innervation, digits maintain the ability to regenerate after re-amputation. Taken together, these data indicate that nerve regeneration is impaired in the context of mouse digit tip regeneration.

1. Introduction

In amphibians, peripheral nerves are highly regenerative and required for the urodele limb regeneration response (Kumar and Brockes, 2012; Stocum, 2011; Todd, 1823). Peripheral nerves are thought to stimulate regeneration via the release of neurotrophic factors including transferrin (Kiffmeyer et al., 1991), FGFs (Satoh et al., 2011), anterior gradient protein (Kumar et al., 2007), neuregulin-1 (Farkas et al., 2016), and BMPs (Makanae et al., 2014). Implanting certain neurotrophic molecules such as neuregulin-1 (Farkas et al., 2016), combinations of FGFs and BMPs (Makanae et al., 2014), or dorsal root ganglia can rescue limb regeneration after denervation (Goldhamer et al., 1992; Kamrin and Singer, 1959; Tomlinson and Tassava, 1987). Additional evidence for a peripheral nerve requirement for limb regeneration come from gain-of-function experiments in which an accessory limb can be formed from a simple skin wound by rerouting nerves to the injury and adding a contralateral piece of dermis (Endo et al., 2004; Makanae and Satoh, 2012; Satoh et al., 2015).

Mice and humans are capable of regenerating the distal tip of their toes and fingers, respectively (Dolan et al., 2018; Douglas, 1972; Illingworth, 1974). In mice, inflammatory cells and osteoclasts are recruited to the injury after amputation and act to remove pathogens and to degrade dead bone (Simkin et al., 2015, 2017). When the amputation wound heals, a blastema forms between the proximal bone stump and distal epidermis. The blastema is a transient, highly proliferative, heterogeneous, and lineage-restricted collection of stem/progenitors cells that organizes the regeneration response (Han et al., 2003; Lehoczky et al., 2011; Muneoka et al., 2008; Rinkevich et al., 2011). Epimorphic regeneration, defined by the formation of a

* Correspondence to: Physiology and Pharmacology, College of Veterinary Medicine and Biomedical Sciences, Texas A & M University, College Station, TX 77843, USA.
E-mail addresses: cpdolan@cvm.tamu.edu (C.P. Dolan), myan@cvm.tamu.edu (M. Yan), kzimmel@cvm.tamu.edu (K. Zimmel), teejyay@tamu.edu (T.-J. Yang), eleininger@tulane.edu (E. Leininger), ldawson@cvm.tamu.edu (L.A. Dawson), kmuneoka@cvm.tamu.edu (K. Muneoka).

https://doi.org/10.1016/j.ydbio.2018.11.010
Received 3 October 2018; Received in revised form 12 November 2018; Accepted 15 November 2018
Available online 17 November 2018
0012-1606/

blastema, distinguishes complex multi-tissue regeneration from tissue-specific regeneration responses (e.g. fracture repair, liver regeneration, etc.). By four weeks after injury, amputated structures—including bone, nail, epidermis, and vasculature—have completely regenerated. However, regeneration is restricted to the distal digit tip, and amputation at more proximal levels results in bone truncation, fibrotic healing and scar formation (Dawson et al., 2016; Yu et al., 2010). Similar to the salamander limb, mouse digit tip regeneration is a peripheral nerve-dependent event (Johnston et al., 2016; Rinkevich et al., 2014; Takeo et al., 2013), however unlike amphibians, transected mammalian peripheral nerves exhibit regenerative deficits (Jonsson et al., 2013). Nevertheless, transection of the sciatic nerve before digit tip amputation inhibits digit tip regeneration (Johnston et al., 2016; Rinkevich et al., 2014; Takeo et al., 2013). Schwann cells have also been implicated in digit tip regeneration, and supplementing a denervated digit with PDGF-AA or Oncostatin-M can rescue the denervated regenerative response (Johnston et al., 2016).

The mammalian peripheral nervous system is a complex organ, comprised of numerous subtypes of nerves and Schwann cells that each have a specific function. Presently, it is unknown what types of nerves and Schwann cells innervate the digit tip, and to what extent these cells regenerate in association with the regenerative response. Given the necessity of peripheral nerves for mammalian regeneration, it is critical to address this gap in knowledge. Here, we characterize the neuroanatomy of the unamputated digit tip and show that there is a significant reduction of both nerves and Schwann cells in the regenerated digit tip. These findings suggest that the neurotrophic requirement for regeneration is fundamentally different in mammals versus amphibians.

2. Materials and methods

2.1. Animals and amputations

Adult 8-week-old, female CD-1 mice were purchased from Texas Institute for Genomic Medicine. Digit tip amputations of the 2nd and 4th hindlimb digits were performed as described previously (Simkin et al., 2013). In some mice regenerated digits were re-amputated. All animal use and techniques were in compliance with the standard operating procedures of Texas A & M University's Institutional Animal Care and Use Committee.

2.2. Digit processing and histological staining

Digits were collected from mice and fixed in buffered zinc formalin (Anatech Ltd) for 24 h at room temperature. Digits were decalcified using Decalcifier I (Surgipath), a 10% formic acid solution, for 24 h. Decalcified digits were embedded in paraffin, serially sectioned (4–5 μm) and mounted onto microscope slides. For histological staining, slides were incubated at 60 °C (45 min), 37 °C (2 h), deparaffinized to water and stained with Mallory trichrome. Slides were mounted using Permount Mounting Medium (Thermo Fisher Scientific). All slides were imaged using either 1) Olympus BX60 microscope with an Olympus DP72 camera, utilizing the DP2-BSW software, or 2) the Olympus VS120 microscope with a Pike F-505C camera (Allied Vision) utilizing the VS-ASW FL2.8 software.

2.3. Immunohistochemistry

Antigen retrieval was performed using heat retrieval performed in citrate buffer solution (Dako). Slides were blocked using Protein Block (Dako) for 1 h at room temperature. Incubation with primary antibody was performed overnight at 4 °C; followed by a wash in tris buffered saline with Tween R20 solution (Sigma-Aldrich Co.) and incubated in secondary antibody for 1 h at room temperature. Slides were then incubated in a phosphate buffered saline (Sigma-Aldrich) and DAPI (Invitrogen) solution, dried, and mounted with Prolong Gold (Invitrogen). Samples were imaged using the either 1) Olympus BX61 microscope with a Hamamatsu ORCA-ER camera via the Slidebook software (Intelligent Imaging Innovations Inc.) or 2) Olympus VS120 microscope with a Hamamatsu ORCA-Flash4.0 V2 Digital CMOS camera via VS-ASW FL2.8 software (Olympus). Primary antibodies used were chicken anti-glial fibrillary acidic protein (1:500; Abcam; Ab4674), chicken anti-neurofilament H (1:1000; Millipore; Ab5539), guinea pig anti-substance P (1:250; Abcam; Ab10353), rabbit anti-tyrosine hydroxylase (1:500; Abcam; Ab112), rabbit anti-beta III tubulin (1:500; Abcam; Ab18207), and rabbit anti-protein zero (1:1000; Millipore; Abn363). Secondary antibodies used were goat anti-rabbit, chicken, or guinea pig Alexa Fluor-488, 568 or 647 (1:500; Invitrogen).

2.4. Quantification of β3T, P0, and GFAP

Quantitation of immunostained sections was carried out for β3T in the bone marrow and distal tip, and for P0 and GFAP in the connective tissue. 4–8 samples were analyzed and 3 images per sample were averaged for each region of interest. The region of interest was identified (μm^2) and images were acquired at 200X magnification. The immunofluorescent signal identified the area of antibody staining (μm^2) and this was normalized to the region of interest. For statistical analysis, either an unpaired *t*-test or a one-way ANOVA with a post-hoc Tukey's multiple comparisons test was performed using GraphPad Prism 7 software (GraphPad Software).

2.5. Micro-computed tomography (μCT), repeat amputations, and quantification of P3 bone volume and length

μCT scanning was performed using a vivaCT 40 (SCANCO Medical) as previously described (Fernando et al., 2011). For the first amputation, unamputated (0DPA), amputated (1DPA), and regenerated (28DPA) digits were scanned. Immediately after scanning regenerated digits, mice were anesthetized as described above, and the distal tip of their digits were re-amputated. The following day, amputated digits (1DPA(2)) were scanned, allowed to regenerated for four weeks, and then were scanned to assess regeneration (28DPA(2)). Using GraphPad Prism 7 software, a repeated-measures one-way ANOVA with a post-hoc Tukey's multiple comparisons test was used to assess statistical significance.

3. Results

3.1. Neuroanatomy of the unamputated digit tip

The terminal phalanx (P3) of the 2nd and 4th hindlimb digits are each innervated by two nerves (digital nerves) that extend the length of the digit and are positioned ventrolaterally to the three phalangeal elements (P1, P2, P3; Fig. 1A). Axons are identified based on immunostaining for the pan-neuronal markers beta-III-tubulin (β3T) and neurofilament-H (NFH) and these markers are expressed in digital nerve axons (Fig. 1B; Supp. Fig. 1A-D). While all digit samples analyzed co-express both neuronal markers, β3T expression is more prominent than NFH expression. At the level of the os holes, two prominent skeletal foramens that connect the P3 bone marrow cavity with the surrounding connective tissue, each digital nerve bifurcates to establish two distinct branches: one that innervates the bone marrow (BM branch) (Fig. 1C; Supp. Fig. 1E-G) via the os hole, and another that remains peripheral to the P3 element and innervates the surrounding connective tissue (CT branch) (Fig. 1D; Supp. Fig. 1F,G). The BM branches terminate onto vasculature within the P3 marrow compartment (Fig. 1C; Supp. Fig. 1F,G). The CT branches extend distal and dorsal through tissues surrounding the P3 bone and extend axons that project to epidermal structures (Fig. 1E; Supp. Fig. 1H) including the nailbed (Fig. 1F).

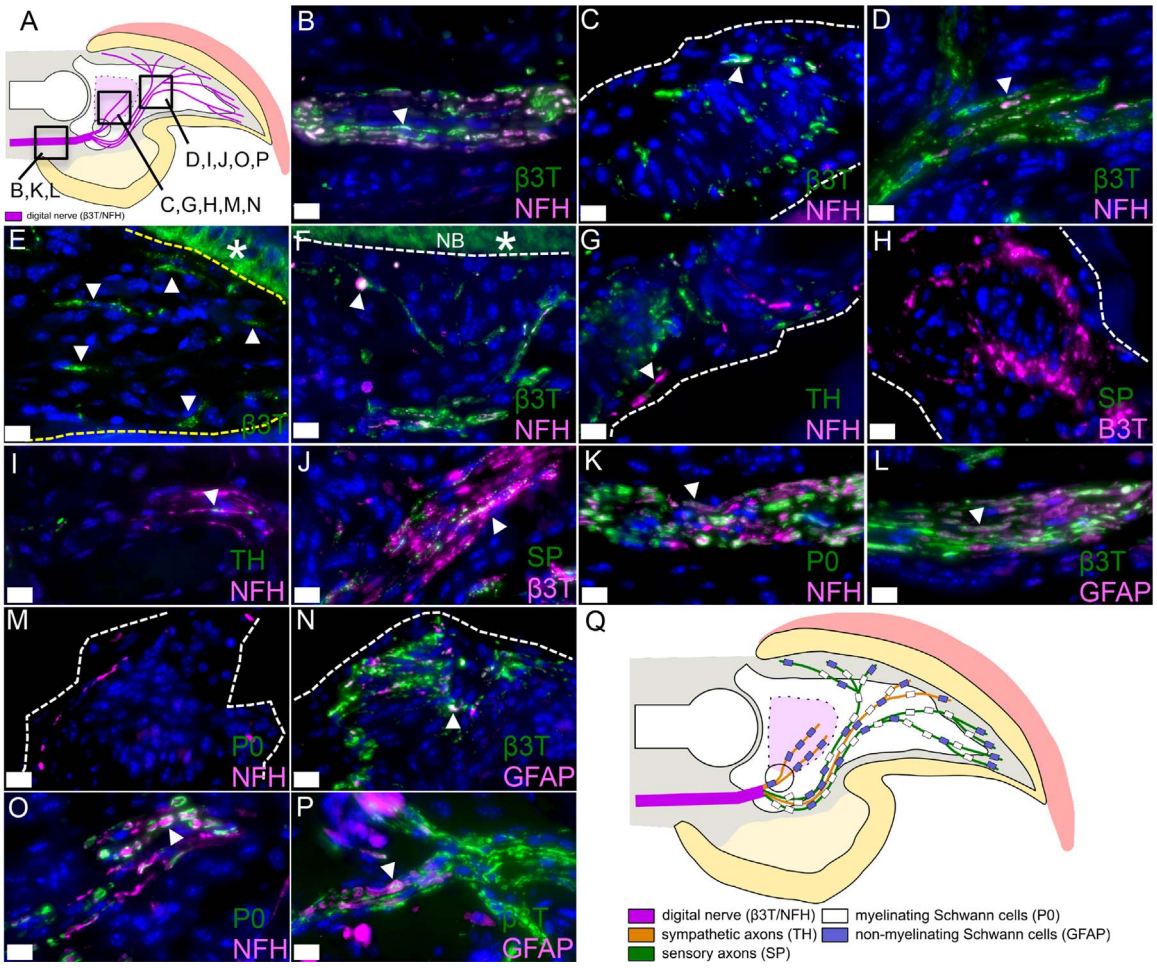

Fig. 1. Neuroanatomy of the Unamputated Digit Tip. (A) Diagram of the digital nerves in the terminal phalanx (P3). The black boxes indicate where images were taken within the P3 region with letters corresponding to the other images in the figure. **(B-F)** β3T and NFH immunopositive axons (arrowheads) in the proximal digital nerves **(B)**, BM branch **(C)**, CT branch **(D)**, the distal digit tip **(E)**, and subjacent to the nailbed **(F)**. Arrowheads indicate axons; * indicate β3T-immunopositive keratinocytes in the nail bed. **(G)** Expression of TH and NFH (arrowhead) indicating that the BM branches are composed of sympathetic axons. **(H)** SP immunopositive axons are absent from the BM branches. **(I)** Expression of TH and NFH (arrowhead) indicating that the CT branches are composed of sympathetic axons. **(J)** Expression of SP and β3T (arrowhead) indicating that the CT branches are composed of sensory axons. **(K)** P0 myelinating-Schwann cells associate with NFH axons (arrowhead) in the digital nerves. **(L)** GFAP non-myelinating-Schwann cells associate with β3T axons (arrowhead) in the digital nerves. **(M)** P0 myelinating-Schwann cells are not associated with BM branch axons. **(N)** GFAP non-myelinating-Schwann cells associate with BM branch axons (arrowhead). **(O)** P0 myelinating-Schwann cells associate with CT branch axons (arrowhead). **(P)** GFAP non-myelinating-Schwann cells associate with CT branch axons (arrowhead). **(Q)** Diagram of the complete neuroanatomy of the terminal phalanx. β3T: beta-3-tubulin; NFH: neurofilament-H; TH: tyrosine hydroxylase; SP: substance P; P0: myelin protein zero; GFAP: glial fibrillary acidic protein; BM: bone marrow; CT: connective tissue; NB: nailbed. Scale bar = 10 μm. White dashed lines: delineates BM vasculature; Yellow dashed lines: delineates epidermis.

The peripheral nervous system (PNS) is heterogeneous in composition, consisting of a number of axonal subtypes including sympathetic, sensory, and motor neurons. The axons of sympathetic neurons can be identified based on expression of tyrosine hydroxylase (TH) (Lazaroff et al., 1995), sensory neurons based on expression of substance P (SP) (Harrison and Geppetti, 2001), and motor neurons based on expression of choline acetyl-transferase (ChAT) (Misgeld et al., 2002). Coupling one of the pan-neuronal antibodies with subtype specific axonal immunostaining we are able to identify the composition of the BM and CT branches of the digital nerves. Since the digit does not contain any muscle tissue, it is not surprising that $ChAT^{+}$ axons are not observed in the digit tip (data not shown). BM branch axons are immunopositive for TH (100%; n = 7/7) and the minority of digits are immunopositive for SP (14%; n = 1/7) indicating that they are sympathetic and not sensory (Fig. 1G,H). Conversely, CT branch axons are immunopositive for both TH (86%; n = 6/7) and SP (100%; n = 7/7) indicating that the CT branch contains both sympathetic and sensory axons (Fig. 1J). CT branch axons that are SP immunopositive terminate at epidermal structures whereas TH immunopositive axons appear to terminate on vasculature.

Schwann cells play a critical role in PNS function, and recently have been shown to be required for digit tip regeneration (Johnston et al., 2016). Within the PNS there are two types of terminally-differentiated Schwann cells: 1) Myelinating-Schwann cells ensheathe a single axon, are critical for proper conduction of nerve impulses and can be identified based on expression of myelin protein zero (P0), a glycoprotein expressed in the myelin sheath (Salzer, 2015); 2) Non-myelinating-Schwann cells ensheathe multiple axons, are commonly found at axon termini and can be identified based on expression of glial fibrillary acidic protein (GFAP), an intermediate filament protein (Jessen et al., 1990). Coupling one of the pan-neuronal antibodies with Schwann cell-specific immunostaining we characterized the BM and CT branches of the digital nerves. The digital nerves proximal to the digital nerve bifurcation are immunopositive for both P0 and GFAP, indicating that this region is associated with both myelinating and non-myelinating Schwann cells (Fig. 1K,L). BM branch axons are associated with cells immunonegative for P0, but immunopositive for GFAP, indicating that they are only associated with non-myelinating-Schwann cells (Fig. 1M,N). CT branch axons are immunopositive for both P0 and GFAP indicating that, like the proximal digital nerve, they are

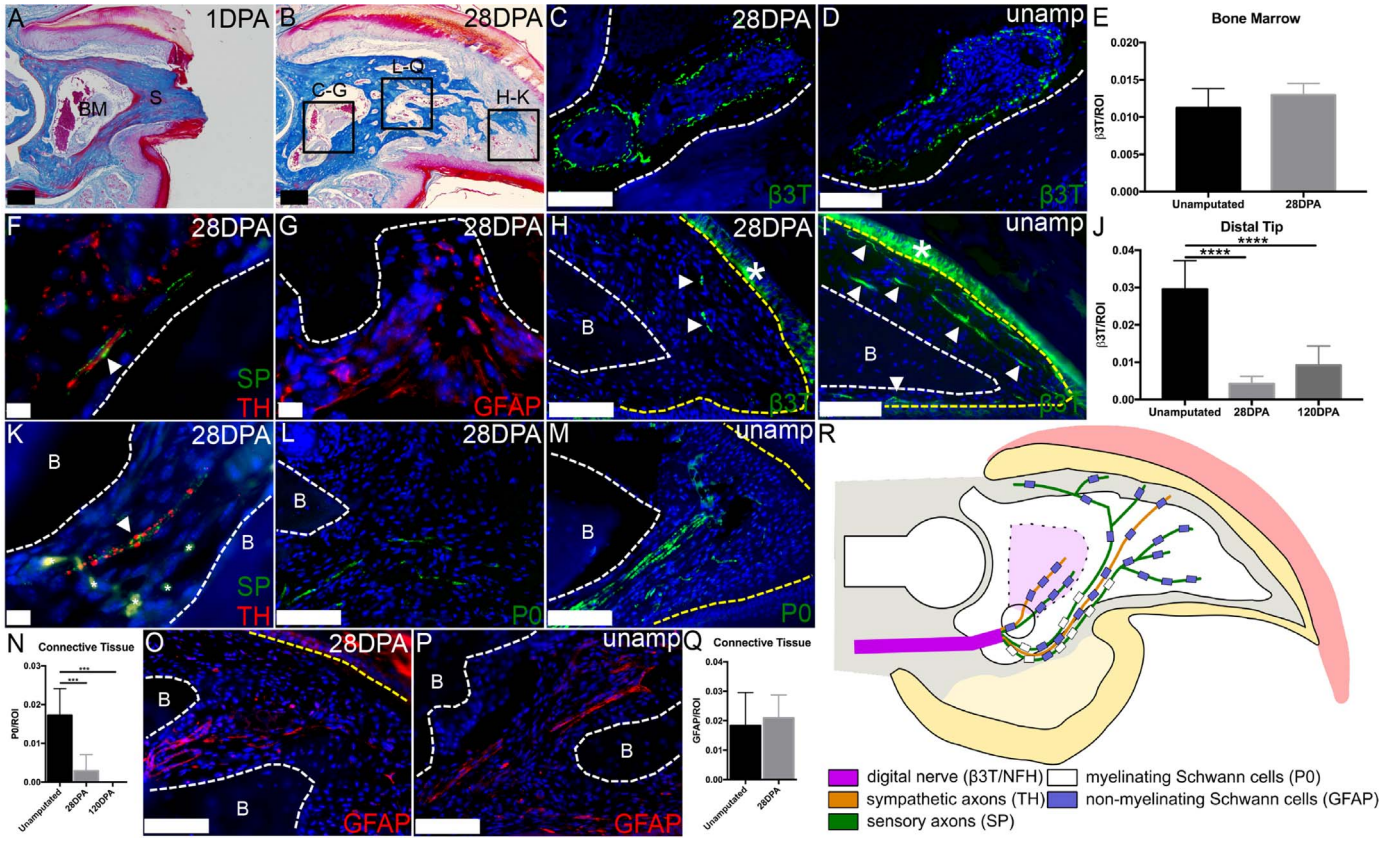

Fig. 2. Neuroanatomy of the Regenerated Digit Tip. (A,B) Mallory's Trichrome staining of the amputated digit at 1 DPA **(A)** and regenerated digit at 28 DPA **(B). (C,D)** β3T immunopositive axons in the BM of the regenerated **(C)** and unamputated digit **(D). (E)** Quantification of β3T immunopositive axons in the BM (mean ± SD; n=8; P=0.1239). **(F)** SP (arrowheads) and TH immunopositive axons in the BM of the regenerated digit. **(G)** GFAP immunopositive non-myelinating-Schwann cells in the BM of the regenerated digit. **(H,I)** β3T immunopositive axons in the distal digit tip of the regenerated **(H)** and unamputated digit **(I)**. Arrowheads indicate axons; * indicate β3T-immunopositive keratinocytes in the nail bed. **(J)** Quantification of β3T immunopositive axons in the unamputated and regenerated distal digit tip at 28 and 120 DPA (mean ± SD; n=5–8; **** = P < 0.0001). **(K)** SP and TH immunopositive axons in the distal tip of the regenerated digit (white asterisks: autofluorescence from red blood cells). **(L,M)** P0 immunopositive myelinating-Schwann cells in CT of the regenerated **(L)** and unamputated **(M)** digit tip. **(N)** Quantification of P0 immunopositive myelinating-Schwann cells in the CT of the unamputated and regenerated digit tip at 28 and 120 DPA (mean ± SD; n=4–7; *** = P < 0.001) **(O,P)** GFAP immunopositive non-myelinating-Schwann cells in the CT of the regenerated **(O)** and unamputated **(P)** digit tip. **(Q)** Quantification of GFAP immunopositive non-myelinating-Schwann cells in the CT of the unamputated and regenerated digit (mean ± SD; n=6–7; P=0.63). **(R)** Diagram of the neuroanatomy of the regenerated terminal phalanx. β3T: beta-3-tubulin; NFH: neurofilament-H; TH: tyrosine hydroxylase; SP: substance P; P0: myelin protein zero; GFAP: glial fibrillary acidic protein; S: stump bone; BM: bone marrow; CT: connective tissue; B: bone; unamp: unamputated digit; DPA: days post amputation **A**,**B**: Scale bar = 200 μm. **C**,**D**,**H**,**I**,**L**,**M**,**O**,**P**: Scale bar = 100 μm. **F**,**G**,**K**: Scale bar = 10 μm. **C**,**D**,**F**,**G**: White dashed lines: delineates BM vasculature; **H**,**I**,**L**,**M**,**O**,**P**: White dashed lines: delineates P3 bone; **H**,**I**: Yellow dashed lines: delineates epidermis.

associated with myelinating and non-myelinating Schwann cells (Fig. 1O,P).

In summary (Fig. 1Q), the digit tip is innervated by two ventro-lateral digital nerves that each bifurcate at the base of the P3 bone. The BM branches enter the P3 marrow through the os holes and consist of sympathetic axons associated with non-myelinating Schwann cells that terminate on marrow vasculature. The CT branches consist of sensory axons that terminate on the epidermal structures and sympathetic axons that terminate on vasculature, and that associate with myelinating and non-myelinating Schwann cells. These data identify clear differences in axon and Schwann cell composition that correlate with physiological functions expected in different regions of the digit tip.

3.2. Neuroanatomy of the regenerated digit tip

Amputation of the digit tip removes approximately 25% of the P3 bone length as well as the surrounding connective tissues, skin, nail, vasculature, and axons of the CT branches, but leaves the marrow region intact (Fig. 2A). During the regenerative response however, the stump bone surrounding the marrow is degraded and the blastema forms from an intermingling of marrow and connective tissue cells (Dawson et al., 2018). Thus, the proximal region of the blastema is contiguous peripherally with the stump connective tissue, and centrally with the distal bone marrow. Twenty-eight days post-amputation (DPA) the bone marrow is restored as is the P3 bone length (Fig. 2B) (Dawson et al., 2018; Fernando et al., 2011). While the amputated P3 bone is cortical, the regenerate consists of woven bone that contains numerous vascularized pockets that are contiguous with the marrow region and the surrounding connective tissue (Fig. 2B). To assess how the neuroanatomy of the digit tip had changed during regeneration, we analyzed 28 DPA regenerates and immunostained for axon and Schwann cell markers (Fig. 2; Supp. Fig. 2).

The BM branch of the digital nerve innervates the regenerated P3 marrow and axons are immunopositive for β3T. Quantitative analysis comparing β3T expression of representative sections of the marrow region between regenerates and unamputated control digits show that the average β3T expression in the regenerates (0.013 ± 0.0005; n = 8) was similar to controls (0.011 ± 0.001; n = 8; P = 0.1239) (Fig. 2C-E). Similar to the unamputated digit, axons of the BM branch are immunopositive for TH (100%; n = 12/12) (Fig. 2F). However, in 50% of regenerated digits (n = 6/12) SP immunopositive sensory axons are also observed in the bone marrow compartment (Fig. 2F). Schwann cells in the BM are immunopositive for GFAP (Fig. 2G) and immunonegative for P0 (data not shown), indicating similarity to the unamputated controls.

Digit tip amputation transects CT branch axons and removes the

distal tissue that these axons innervate. The regenerated digit tip contains axons that track to the CT branch of the digital nerve however, they do not appear as abundant when compared to control unamputated digits, particularly when considering innervation of the epidermis (Fig. 2H,I). Quantitative analysis of axons within the connective tissue of the digit tip indicates that the distal tip of the regenerate contains significantly fewer axons when compared to unamputated control digit tips (Fig. 2J). The average β3T expression in control digits was 0.03 ± 0.003 (n = 6) whereas the average β3T expression in regenerated digits was 0.004 ± 0.0007 (n = 8; P < 0.0001) indicating a 7.5-fold decline in the ability to restore digit innervation (Fig. 2J). To determine if axon regrowth is delayed in digit tip regeneration, we analyzed digits at 120 DPA and found that the average β3T expression in regenerated digits was 0.009 ± 0.002 (n = 5; P < 0.0001) indicating a 3.3-fold decline (Fig. 2J). These data demonstrate that axon regeneration associated with digit tip regeneration is impaired and not simply delayed. SP immunopositive sensory axons are observed in all of the regenerated digits (100%; n = 12/12) whereas TH immunopositive sympathetic axons are only observed in 42% of regenerated digits (n = 5/12) (Fig. 2K). Associated with the decrease in regenerated axons the average level of P0 expression in regenerated digits (0.003 ± 0.002; n = 7) was significantly lower than unamputated control digits (0.017 ± 0.003; n = 4; P < 0.001) at 28 DPA (Fig. 2L-N). This 5.6-fold decline in myelinated Schwann cells correlates with the 7.5-fold decline in regenerated axons and suggest that the reduced number of regenerated sensory axons are appropriately myelinated. Moreover, P0-immunopositive myelinating Schwann cells in the regenerated digit at 120 DPA have not regenerated back to unamputated levels ($4.46e^{-5}$ ± $1.43e^{-5}$; n = 5; P < 0.0001) (Fig. 2N). Conversely, the average level of GFAP expression in regenerated digits (0.021 ± 0.003; n = 7) was not significantly different when compared to unamputated control digits (0.018 ± 0.005; n = 6; P = 0.63), indicating that the non-myelinating Schwann cell population is restored during regeneration (Fig. 2O-Q).

In summary (Fig. 2R), after regeneration BM branch axons remain quantitatively similar to unamputated control digits, although we do observe an increase in sensory axons within the bone marrow compartment. CT branch axons display an impaired regeneration response and there is a significant decrease in myelinating Schwann cells whereas the non-myelinating-Schwann cells regenerate to levels similar to unamputated control digits.

3.3. Neuroanatomy of the blastema

The blastema is a transient structure that forms between the wound epidermis and bone stump and distinguishes digit tip regeneration from tissue-specific regenerative responses in mammals (Fig. 3A) (Seifert and Muneoka, 2018). The blastema is avascular, hypoxic, derived from multiple tissue sources, and is highly proliferative (Dolan et al., 2018). The central region of the blastema is immunonegative for β3T (Fig. 3B) indicating that this blastema region is devoid of axons. Rather, β3T immunopositive axons are restricted to peripheral and distal blastema regions indicating that regenerating axons envelop the central core of proliferating pre-osteogenic blastema cells (Fig. 3B) (Dawson et al., 2018). These regenerating axons are immunopositive for SP and immunonegative for TH (Fig. 3C,D) indicating that the regenerating axons at this stage are sensory. These sensory axons are associated with GFAP but not P0 expressing cells (Fig. 3E,F) indicating that only non-myelinating-Schwann cells are supporting the regenerative response. We note that axons at the distal end of the blastema associated with the wound epidermis are not always associated with Schwann cells (Fig. 3E). TH and SP immunopositive axons are found in the bone marrow (Fig. 3G,H) indicating that both sympathetic and sensory axons are present in the bone marrow during the blastema stage of regeneration. Axons in the bone marrow associate with non-myelinating Schwann cells but not myelinating Schwann cells, similar to the unamputated and regenerated digits. (Fig. 3I,J).

3.4. Re-amputation does not inhibit digit tip regeneration

Since mouse digit tip regeneration has been shown to be peripheral nerve-dependent (Takeo et al., 2013; Rinkevich et al., 2014; Johnston et al., 2016) but the regeneration of digit nerves is impaired, we carried out a quantitative micro-computed tomography (μCT) analysis of regeneration following re-amputation of regenerated digits (Simkin et al., 2015) to determine if a second regenerative response was impaired. Digit tips were amputated and allowed to regenerate for four weeks at which time the regenerated digits were re-amputated and analyzed after four additional weeks. For quantifying P3 bone regeneration, unamputated, amputated, and regenerated digits were scanned using in vivo μCT which allows for monitoring the regeneration responses of the same digit following repeated amputation. Representative μCT redendered-3D images clearly show that regeneration is not inhibited following re-amputation (Fig. 4A). After the first amputation, digits regenerate significantly more bone volume (BV) compared to the unamputated digit (P < 0.0001; n = 39) consistent with a BV overshoot previously reported (Fig. 4B) (Dawson et al., 2018; Fernando et al., 2011). After the second amputation, we observe a similar trend, with a significant increase in BV compared the first regenerate (P < 0.0001; n = 39) and producing a P3 bone volume that is approximately 50% larger than the initial unamputated digit tip (Fig. 4B). These results clearly show that impaired innervation does not restrict the regenerative capabilities of the digit tip.

4. Discussion

The neuroanatomy of the mouse digit tip is largely predicted from innervation studies of the bone marrow and skin in other parts of the body. The digit tip is innervated by two ventrolateral digital nerves that upon reaching the terminal phalanx bifurcate into two distinct branches: the BM and CT branch. The BM branches are composed of sympathetic axons associated with non-myelinating-Schwann cells which is consistent with published bone marrow studies characterizing innervation of the marrow compartment (Bjurholm et al., 1988). The CT branches are composed of sensory and sympathetic axons that associate with myelinating-Schwann cells and non-myelinating-Schwann cells. These data parallel well-established reports that sensory nerves of the dermis are responsible for receiving and transmitting afferent signals while sympathetic nerves regulate vascular tone primarily by inducing vasoconstriction of small resistance arteries (Bruno et al., 2012; Zochodne, 2008). The importance of a detailed assessment of the digit tip axons and Schwann cells rests in the fact that this region of the mammalian limb displays endogenous regenerative properties and that the regenerative response is dependent on both nerves and Schwann cells (Johnston et al., 2016; Rinkevich et al., 2014; Takeo et al., 2013).

One striking result from this study is that successful digit tip regeneration is associated with a reduction of connective tissue axons when compared to unamputated controls. While this finding is consistent with poor regenerative capabilities of mammalian PNS axons following axotomy (Stankovic et al., 1996), the results are not consistent with studies demonstrating that nerves are required for digit tip regeneration (Johnston et al., 2016; Rinkevich et al., 2014; Takeo et al., 2013). Moreover, we show a robust regenerative response in digits with impaired innervation. The neurotrophic effect on epimorphic regeneration has been best studied in salamander limb regeneration where there is robust regeneration of limb axons that produce neurotrophic factors essential for the regeneration response (Pirotte et al., 2016; Satoh et al., 2015). Whether there is a similar neurotrophic effect in mammalian regeneration is important with respect to strategies for enhancing regenerative capabilities, particularly in humans. A number of studies show that regeneration of the denervated digit tip is not completely inhibited, but is associated with a delayed healing response, a reduced level of blastema cell proliferation and delayed/reduced bone regrowth (Mohammad and Neufeld, 2000;

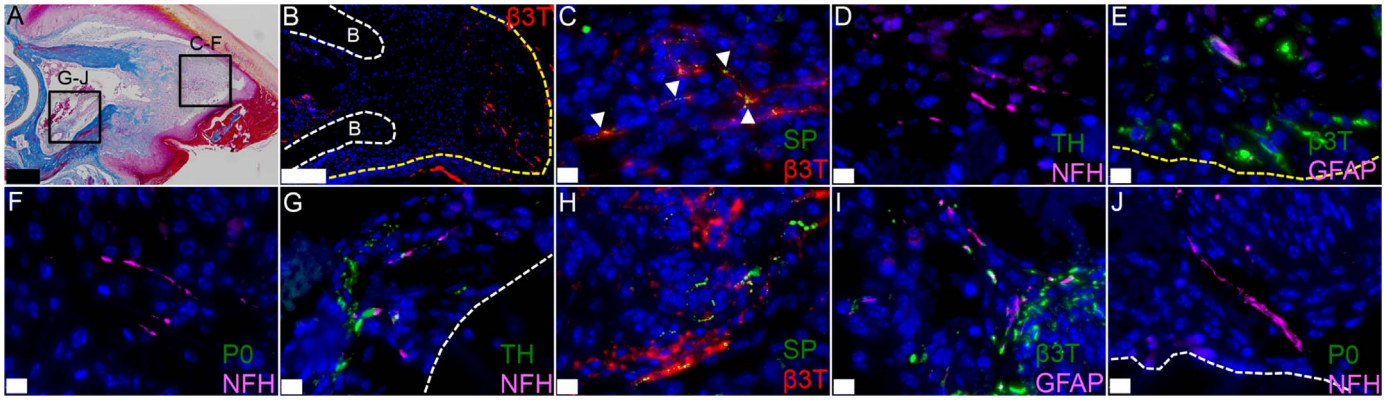

Fig. 3. Neuroanatomy of the Blastema. (A) Mallory's Trichrome staining of the blastema at 10 DPA. **(B-J)** Immunohistochemical staining of the blastema at 10 DPA. **(B)** β3T immunopositive axons surround, but are not found in the center of the blastema. **(C)** Expression of SP (arrowheads) and β3T indicate sensory axons in the distal blastema. **(D)** TH immunopositive sympathetic axons are not found in the distal digit tip. **(E)** GFAP immunopositive non-myelinating-Schwann cells in the distal blastema associated with some but not all β3T immunopositive axons. **(F)** P0 immunopositive myelinating-Schwann cells are not found in the distal blastema. **(G,H)** TH **(G)** and SP **(H)** immunopositive axons are present in the BM at 10 DPA. **(I,J)** GFAP immunopositive non-myelinating-Schwann cells **(I)**, but not P0 immunopositive myelinating-Schwann cells **(J),** are found associated with axons in the BM at 10 DPA. β3T: beta-3-tubulin; NFH: neurofilament-H; TH: tyrosine hydroxylase; SP: substance P; P0: myelin protein zero; GFAP: glial fibrillary acidic protein; BM: bone marrow; CT: connective tissue; B: bone; unamp: unamputated digit; DPA: days post amputation. **C-J**: Scale bars = 100 μm. **C-J**: Scale bars = 10 μm. **B**: White dashed line: delineates terminal phalanx bone; Yellow dashed lines: delineates epidermis. **G**,**J**: White dashed lines: delineates BM vasculature.

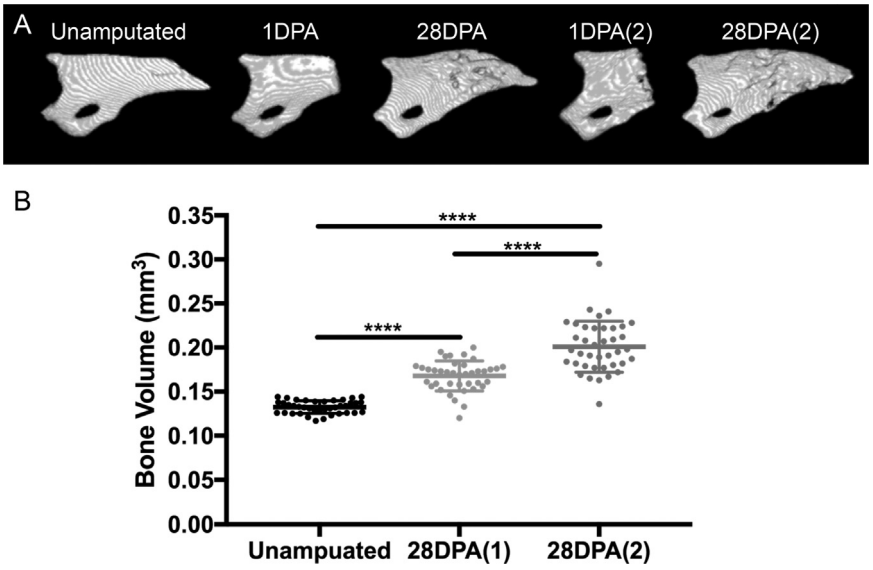

Fig. 4. Re-amputation does not inhibit digit tip regeneration (A) Representative μCT redendered-3D images of the unampuated, amputated (1DPA), regenerated (28DPA), re-amputated (1DPA(1)), and 2nd regeneration ((28DPA(2)) P3 digit bone. **(B)** Quantitative measurements of P3 digit bone volume. **** = P < 0.0001. DPA = Days post amputation.

Rinkevich et al., 2014; Takeo et al., 2013). The central region of the digit blastema is osteogenic and highly proliferative (Dawson et al., 2018), and we show here that it is also devoid of axons making it unlikely that proliferation of pre-osteoblasts within the blastema is a nerve-dependent event. This conclusion is consistent with reports that bone repair is nerve-independent (Miura et al., 2015). Mammalian regeneration studies utilize transection of the sciatic nerve at the level of the thigh to denervate the digit tip, but damaging the sciatic nerve also paralyzes the hindlimb making it non-functional. This procedure can have multiple off-target effects beyond digit denervation; indeed, sciatic nerve transection is commonly used to study the effect of activity and mechanical load on limb muscle and skeletal tissues (Gross et al., 2010). Thus, it is possible that the nerve influence on mouse digit tip regeneration is indirect and not necessarily related to the absence of regenerating axons during the response. Overall, it is difficult to find clear parallels between the nerve-dependent responses of salamander limb regeneration and mouse digit regeneration, and the available evidence supports the conclusion that there are fundamental differences in the neurotrophic influence on these two epimorphic regeneration models (Mohammad and Neufeld, 2000).

Schwann cells are known to be present during the digit tip regenerative response where they produce PDGF and Oncostatin-M that are both mitogenic for blastema cells (Johnston et al., 2016). In response to PNS axon injury, Schwann cells are known to support and guide the regrowth of severed axons by the modification the wound environment and the production of specific trophic factors (Boyd and Gordon, 2003; Chen et al., 2007; Scheib and Hoke, 2013; Wood and Mackinnon, 2015). Thus, it is conceivable that the digit tip regenerative response has evolved mechanisms that utilize trophic activities produced by these cells. Nevertheless, there is an overall decline in Schwann cells associated with the regeneration response and only non-myelinating Schwann cells are present during the blastema stage. After peripheral nerve injury, myelinating Schwann cells are known to down-regulate genes associated with myelination (e.g. P0, MBP, MAG, etc.) and up-regulate genes associated with immature and/or non-myelinating Schwann cells (e.g. GFAP, L1, NCAM, etc.) (Chen et al., 2007; Jessen and Mirsky, 2008), thus the absence of myelinating Schwann cells can be attributed to this transformation (Gomez-Sanchez et al., 2017). The restoration of myelinating Schwann cells in the regenerate to numbers that correspond to the reduction in

regenerated CT branch axons suggest that myelinating Schwann cells are re-differentiating in accord with axon maturation. The restoration of non-myelinating Schwann cells to pre-amputation numbers despite a significant decline in regenerated axons is more difficult to explain, and suggests that this population of cells is not responding to the regenerated neural environment, but perhaps to the regenerated vascular environment.

The digit blastema is devoid of vasculature and is hypoxic (Fernando et al., 2011; Sammarco et al., 2014). Maintaining the blastema in a hypoxic state plays a critical role in coordinating the regenerative response (Sammarco et al., 2015; Simkin et al., 2015). We show here that the avascular region of the blastema is also devoid of axons and Schwann cells, and this is suggestive that the regenerative responses of these tissues are somehow linked. During digit tip regeneration, blastema cells express *Pedf*, a potent anti-angiogenic factor that inhibits expression of *Vegf*, which creates a pro-regenerative wound environment by inhibiting early revascularization (Yu et al., 2014). Angiogenesis during the healing of full thickness skin wounds is also modulated by the balance between VEGF and PEDF, and in this model excessive angiogenesis is linked to an anti-regenerative wound environment that ultimately leads to the deposition of scar tissue (DiPietro, 2016; Wietecha et al., 2015). During vertebrate development formation of the vascular system precedes and guides subsequent neural innervation (Bates et al., 2003, 2002). Studies of de novo regeneration of peripheral nerve axons following sciatic nerve transection have found that Schwann cells serve as axonal guides but their migration is directed by blood vessels, and that this multicellular response is initiated by macrophages responding to hypoxia (Cattin et al., 2015). The digit regenerative response is dependent on macrophages which play a crucial role at multiple phases of the regenerative process (Simkin et al., 2017). It is intriguing that the regenerating mouse digit blastema has all of the components identified for a peripheral nerve-specific tissue regenerative response, but in the context of a blastema that coordinates the regeneration of multiple tissue types, including bone, epidermis and connective tissue. Together the evidence suggest that hypoxia and macrophages play a regulatory role in coordinating digit vasculature as well as epidermal and osteogenic regeneration (Simkin et al., 2015, 2017), while Schwann cells and regenerating axons utilize regenerating vascular routes to re-innervate the digit tip.

Acknowledgements

We would like to thank the entire Muneoka lab, Dr. Dana Gaddy, and Dr. Larry Suva for thoughtful discussions and proof reading the manuscript.

Funding

This work was supported by Texas A&M University.

Appendix A. Supporting information

Supplementary data associated with this article can be found in the online version at doi:10.1016/j.ydbio.2018.11.010.

References

Bates, D., Taylor, G.I., Minichiello, J., Farlie, P., Cichowitz, A., Watson, N., Klagsbrun, M., Mamluk, R., Newgreen, D.F., 2003. Neurovascular congruence results from a shared patterning mechanism that utilizes Semaphorin3A and Neuropilin-1. Dev. Biol. 255, 77–98.

Bates, D., Taylor, G.I., Newgreen, D.F., 2002. The pattern of neurovascular development in the forelimb of the quail embryo. Dev. Biol. 249, 300–320.

Bjurholm, A., Kreicbergs, A., Terenius, L., Goldstein, M., Schultzberg, M., 1988. Neuropeptide Y-, tyrosine hydroxylase- and vasoactive intestinal polypeptide-immunoreactive nerves in bone and surrounding tissues. J. Auton. Nerv. Syst. 25, 119–125.

Boyd, J.G., Gordon, T., 2003. Neurotrophic factors and their receptors in axonal regeneration and functional recovery after peripheral nerve injury. Mol. Neurobiol. 27, 277–324.

Bruno, R.M., Ghiadoni, L., Seravalle, G., Dell'oro, R., Taddei, S., Grassi, G., 2012. Sympathetic regulation of vascular function in health and disease. Front. Physiol. 3, 284.

Cattin, A.L., Burden, J.J., Van Emmenis, L., Mackenzie, F.E., Hoving, J.J., Garcia Calavia, N., Guo, Y., McLaughlin, M., Rosenberg, L.H., Quereda, V., Jamecna, D., Napoli, I., Parrinello, S., Enver, T., Ruhrberg, C., Lloyd, A.C., 2015. Macrophage-induced blood vessels guide Schwann cell-mediated regeneration of peripheral nerves. Cell 162, 1127–1139.

Chen, Z.L., Yu, W.M., Strickland, S., 2007. Peripheral regeneration. Annu. Rev. Neurosci. 30, 209–233.

Dawson, L.A., Schanes, P.P., Kim, P., Imholt, F.M., Qureshi, O., Dolan, C.P., Yu, L., Yan, M., Zimmel, K.N., Falck, A.R., Muneoka, K., 2018. Blastema formation and periosteal ossification in the regenerating adult mouse digit. Wound Repair Regen..

Dawson, L.A., Simkin, J., Sauque, M., Pela, M., Palkowski, T., Muneoka, K., 2016. Analogous cellular contribution and healing mechanisms following digit amputation and phalangeal fracture in mice. Regeneration 3, 39–51.

DiPietro, L.A., 2016. Angiogenesis and wound repair: when enough is enough. J. Leukoc. Biol. 100, 979–984.

Dolan, C.P., Dawson, L.A., Muneoka, K., 2018. Digit tip regeneration: merging regeneration biology with regenerative medicine. Stem Cells Transl. Med. 7, 262–270.

Douglas, B.S., 1972. Conservative management of guillotine amputation of the finger in children. Aust. Paediatr. J. 8, 86–89.

Endo, T., Bryant, S.V., Gardiner, D.M., 2004. A stepwise model system for limb regeneration. Dev. Biol. 270, 135–145.

Farkas, J.E., Freitas, P.D., Bryant, D.M., Whited, J.L., Monaghan, J.R., 2016. Neuregulin-1 signaling is essential for nerve-dependent axolotl limb regeneration. Development 143, 2724–2731.

Fernando, W.A., Leininger, E., Simkin, J., Li, N., Malcom, C.A., Sathyamoorthi, S., Han, M., Muneoka, K., 2011. Wound healing and blastema formation in regenerating digit tips of adult mice. Dev. Biol. 350, 301–310.

Goldhamer, D.J., Tomlinson, B.L., Tassava, R.A., 1992. Ganglia implantation as a means of supplying neurotrophic stimulation to the newt regeneration blastema: cell-cycle effects in innervated and denervated limbs. J. Exp. Zool. 262, 71–80.

Gomez-Sanchez, J.A., Pilch, K.S., van der Lans, M., Fazal, S.V., Benito, C., Wagstaff, L.J., Mirsky, R., Jessen, K.R., 2017. After nerve injury, lineage tracing shows that myelin and Remak Schwann cells elongate extensively and branch to form repair Schwann cells, which shorten radically on remyelination. J. Neurosci.: Off. J. Soc. Neurosci. 37, 9086–9099.

Gross, T.S., Poliachik, S.L., Prasad, J., Bain, S.D., 2010. The effect of muscle dysfunction on bone mass and morphology. J. Musculoskelet. Neuron. Interact. 10, 25–34.

Han, M., Yang, X., Farrington, J.E., Muneoka, K., 2003. Digit regeneration is regulated by Msx1 and BMP4 in fetal mice. Development 130, 5123–5132.

Harrison, S., Geppetti, P., 2001. Substance p. Int. J. Biochem. Cell Biol. 33, 555–576.

Illingworth, C.M., 1974. Trapped fingers and amputated finger tips in children. J. Pediatr. Surg. 9, 853–858.

Jessen, K.R., Mirsky, R., 2008. Negative regulation of myelination: relevance for development, injury, and demyelinating disease. Glia 56, 1552–1565.

Jessen, K.R., Morgan, L., Stewart, H.J., Mirsky, R., 1990. Three markers of adult non-myelin-forming Schwann cells, 217c(Ran-1), A5E3 and GFAP: development and regulation by neuron-Schwann cell interactions. Development 109, 91–103.

Johnston, A.P., Yuzwa, S.A., Carr, M.J., Mahmud, N., Storer, M.A., Krause, M.P., Jones, K., Paul, S., Kaplan, D.R., Miller, F.D., 2016. Dedifferentiated schwann cell precursors secreting paracrine factors are required for regeneration of the mammalian digit tip. Cell Stem Cell 19, 433–448.

Jonsson, S., Wiberg, R., McGrath, A.M., Novikov, L.N., Wiberg, M., Novikova, L.N., Kingham, P.J., 2013. Effect of delayed peripheral nerve repair on nerve regeneration, Schwann cell function and target muscle recovery. PLoS One 8, e56484.

Kamrin, A.A., Singer, M., 1959. The growth influence of spinal ganglia implanted into the denervated forelimb regenerate of the newt, Triturus. J. Morphol. 104, 415–439.

Kiffmeyer, W.R., Tomusk, E.V., Mescher, A.L., 1991. Axonal transport and release of transferrin in nerves of regenerating amphibian limbs. Dev. Biol. 147, 392–402.

Kumar, A., Brockes, J.P., 2012. Nerve dependence in tissue, organ, and appendage regeneration. Trends Neurosci. 35, 691–699.

Kumar, A., Godwin, J.W., Gates, P.B., Garza-Garcia, A.A., Brockes, J.P., 2007. Molecular basis for the nerve dependence of limb regeneration in an adult vertebrate. Science 318, 772–777.

Lazaroff, M., Patankar, S., Yoon, S.O., Chikaraishi, D.M., 1995. The cyclic AMP response element directs tyrosine hydroxylase expression in catecholaminergic central and peripheral nervous system cell lines from transgenic mice. J. Biol. Chem. 270, 21579–21589.

Lehoczky, J.A., Robert, B., Tabin, C.J., 2011. Mouse digit tip regeneration is mediated by fate-restricted progenitor cells. Proc. Natl. Acad. Sci. USA 108, 20609–20614.

Makanae, A., Mitogawa, K., Satoh, A., 2014. Co-operative Bmp- and Fgf-signaling inputs convert skin wound healing to limb formation in urodele amphibians. Dev. Biol. 396, 57–66.

Makanae, A., Satoh, A., 2012. Early regulation of axolotl limb regeneration. Anat. Rec. 295, 1566–1574.

Misgeld, T., Burgess, R.W., Lewis, R.M., Cunningham, J.M., Lichtman, J.W., Sanes, J.R., 2002. Roles of neurotransmitter in synapse formation: development of neuromuscular junctions lacking choline acetyltransferase. Neuron 36, 635–648.

Miura, S., Takahashi, Y., Satoh, A., Endo, T., 2015. Skeletal callus formation is a nerve-independent regenerative response to limb amputation in mice and Xenopus. Regeneration 2, 202–216.

Mohammad, K.S., Neufeld, D.A., 2000. Denervation retards but does not prevent toetip

regeneration. Wound Repair Regen.: Off. Publ. Wound Heal. Soc. Eur. Tissue Repair Soc. 8, 277–281.
Muneoka, K., Allan, C.H., Yang, X., Lee, J., Han, M., 2008. Mammalian regeneration and regenerative medicine. Birth Defects Res. Part C Embryo Today: Rev. 84, 265–280.
Pirotte, N., Leynen, N., Artois, T., Smeets, K., 2016. Do you have the nerves to regenerate? The importance of neural signalling in the regeneration process. Dev. Biol. 409, 4–15.
Rinkevich, Y., Lindau, P., Ueno, H., Longaker, M.T., Weissman, I.L., 2011. Germ-layer and lineage-restricted stem/progenitors regenerate the mouse digit tip. Nature 476, 409–413.
Rinkevich, Y., Montoro, D.T., Muhonen, E., Walmsley, G.G., Lo, D., Hasegawa, M., Januszyk, M., Connolly, A.J., Weissman, I.L., Longaker, M.T., 2014. Clonal analysis reveals nerve-dependent and independent roles on mammalian hind limb tissue maintenance and regeneration. Proc. Natl. Acad. Sci. USA 111, 9846–9851.
Salzer, J.L., 2015. Schwann cell myelination. Cold Spring Harb. Perspect. Biol. 7, a020529.
Sammarco, M.C., Simkin, J., Cammack, A.J., Fassler, D., Gossmann, A., Marrero, L., Lacey, M., Van Meter, K., Muneoka, K., 2015. Hyperbaric oxygen promotes proximal bone regeneration and organized collagen composition during digit regeneration. PLoS One 10, e0140156.
Sammarco, M.C., Simkin, J., Fassler, D., Cammack, A.J., Wilson, A., Van Meter, K., Muneoka, K., 2014. Endogenous bone regeneration is dependent upon a dynamic oxygen event. J. Bone Mineral. Res.: Off. J. Am. Soc. Bone Mineral. Res. 29, 2336–2345.
Satoh, A., makanae, A., Hirata, A., Satou, Y., 2011. Blastema induction in aneurogenic state and Prrx-1 regulation by MMPs and FGFs in Ambystoma mexicanum limb regeneration. Dev. Biol. 355, 263–274.
Satoh, A., Mitogawa, K., Makanae, A., 2015. Regeneration inducers in limb regeneration. Dev. Growth Differ. 57, 421–429.
Scheib, J., Hoke, A., 2013. Advances in peripheral nerve regeneration. Nat. Rev. Neurol. 9, 668–676.
Seifert, A.W., Muneoka, K., 2018. The blastema and epimorphic regeneration in mammals. Dev. Biol. 433, 190–199.
Simkin, J., Han, M., Yu, L., Yan, M., Muneoka, K., 2013. The mouse digit tip: from wound healing to regeneration. Methods Mol. Biol. 1037, 419–435.
Simkin, J., Sammarco, M.C., Dawson, L.A., Tucker, C., Taylor, L.J., Van Meter, K., Muneoka, K., 2015. Epidermal closure regulates histolysis during mammalian (Mus) digit regeneration. Regeneration 2, 106–119.
Simkin, J., Sammarco, M.C., Marrero, L., Dawson, L.A., Yan, M., Tucker, C., Cammack, A., Muneoka, K., 2017. Macrophages are required to coordinate mouse digit tip regeneration. Development 144, 3907–3916.
Stankovic, N., Johansson, O., Hildebrand, C., 1996. Occurrence of epidermal nerve endings in glabrous and hairy skin of the rat foot after sciatic nerve regeneration. Cell Tissue Res. 284, 161–166.
Stocum, D.L., 2011. The role of peripheral nerves in urodele limb regeneration. Eur. J. Neurosci. 34, 908–916.
Takeo, M., Chou, W.C., Sun, Q., Lee, W., Rabbani, P., Loomis, C., Taketo, M.M., Ito, M., 2013. Wnt activation in nail epithelium couples nail growth to digit regeneration. Nature 499, 228–232.
Todd, T.J., 1823. On the process of reproduction of the members of the aquatic salamander. Q. J. Sci. Lit. Arts 16, 84–96.
Tomlinson, B.L., Tassava, R.A., 1987. Dorsal root ganglia grafts stimulate regeneration of denervated urodele forelimbs: timing of graft implantation with respect to denervation. Development 99, 173–186.
Wietecha, M.S., Krol, M.J., Michalczyk, E.R., Chen, L., Gettins, P.G., DiPietro, L.A., 2015. Pigment epithelium-derived factor as a multifunctional regulator of wound healing. Am. J. Physiol. Heart Circ. Physiol. 309, H812–H826.
Wood, M.D., Mackinnon, S.E., 2015. Pathways regulating modality-specific axonal regeneration in peripheral nerve. Exp. Neurol. 265, 171–175.
Yu, L., Han, M., Yan, M., Lee, E.C., Lee, J., Muneoka, K., 2010. BMP signaling induces digit regeneration in neonatal mice. Development 137, 551–559.
Yu, L., Yan, M., Simkin, J., Ketcham, P.D., Leininger, E., Han, M., Muneoka, K., 2014. Angiogenesis is inhibitory for mammalian digit regeneration. Regeneration 1, 33–46.
Zochodne, D.W., 2008. Neurobiology of Peripheral Nerve Regeneration. Cambridge University Press, New York, U.S.A..